2

OFFICE OF NAVAL RESEARCH
Grant No. N00014-91-J-1655
R&T Code 4132058---02

# TECHNICAL REPORT NO. 25

# Langmuir-Blodgett Films of 3-Alkyl Pyrroles Studied by STM

by

W.M. Sigmund, T.S. Bailey and R.S. Duran

Center for Macromolecular Science and Engineering
Department of Chemistry
University of Florida
Gainesville, FL

and

M. Hara, H. Sasabe and W. Knoll

Frontier Research Program
The Institute of Physical and Chemical Research (RIKEN)
Wako
Saitama 351-01
Japan

# REPORT DOCUMENTATION PAGE

*Form Approved*
*OMB No 0704-0188*

**1. AGENCY USE ONLY** *(Leave blank)*

**2. REPORT DATE**
12/9/93

**3. REPORT TYPE AND DATES COVERED**

**4. TITLE AND SUBTITLE**
Langmuir-Blodgett Films of 3-Alkyl Pyrroles Studied by STM

**5. FUNDING NUMBERS**
Grant No. N00014-91-J-1655

**6. AUTHOR(S)**
W.M. Sigmund, T.S. Bailey, R.S. Duran, M. Hara, H. Sasabe, and W. Knoll

**7. PERFORMING ORGANIZATION NAME(S) AND ADDRESS(ES)**
R. S. Duran
Department of Chemistry
University of Florida
Gainesville, Florida 32611

**8. PERFORMING ORGANIZATION REPORT NUMBER**
25

**9. SPONSORING/MONITORING AGENCY NAME(S) AND ADDRESS(ES)**
Dr. Kenneth J. Wynne
Code 1113PO, Office of the Chief of Naval Research
800 North Quincy Street
Arlington, VA 22217-5000
(703) 696-4409

**10. SPONSORING/MONITORING AGENCY REPORT NUMBER**

**11. SUPPLEMENTARY NOTES**
will be submitted to Langmuir

**12a. DISTRIBUTION/AVAILABILITY STATEMENT**

**12b. DISTRIBUTION CODE**

**13. ABSTRACT** *(Maximum 200 words)*

By applying the Langmuir-Blodgett (LB) technique mono- and multilayers of monomers and their polymers were built up on conductive solid substrates for studies with scanning tunneling microscopy (STM). Monomers, mixed monomers and polymer monolayers of 3-alkyl pyrroles were transferred onto freshly cleaved molybdenum disulfide (MoS2) and highly oriented pyrolytic graphite (HOPG). High-quality images of the mono- and multilayers could be observed by STM after annealing. Monolayers of monomer were highly ordered showing orientational and positional correlation of alkyl side chains. Mixtures of pyrroles with different side chain lengths showed phase separation. Polymer monolayers showed high side chain orientation more orthogonal to the surface. From the structures observed on solid substrates (gas-solid interface) conclusions are drawn for the polymerization process and the packing of molecules on the Langmuir-trough (at the gas interface).

**14. SUBJECT TERMS**

**15. NUMBER OF PAGES**

**16. PRICE CODE**

**17. SECURITY CLASSIFICATION OF REPORT**
Unclassified

**18. SECURITY CLASSIFICATION OF THIS PAGE**
Unclassified

**19. SECURITY CLASSIFICATION OF ABSTRACT**
Unclassified

**20. LIMITATION OF ABSTRACT**

Will be submitted to LANGMUIR 11/2/93

# Langmuir-Blodgett Films of 3-Alkyl Pyrroles Studied by STM

W. M. Sigmund[1], T. S. Bailey[1], M. Hara[2], H. Sasabe[2], W. Knoll[2], R. S. Duran[1]

[1]Department of Chemistry and Center for Macromolecular Science and Engineering,

University of Florida, Gainesville, Florida 32611 USA

and

[2]Frontier Research Program, The Institute of Physical and Chemical Research (RIKEN),

Wako, Saitama 351-01, Japan

## Abstract

By applying the Langmuir-Blodgett (LB) technique mono- and multilayers of monomers and their polymers were built up on conductive solid substrates for studies with scanning tunneling microscopy (STM). Monomers, mixed monomers and polymer monolayers of 3-alkyl pyrroles were transferred onto freshly cleaved molybdenum disulfide ($MoS_2$) and highly oriented pyrolytic graphite (HOPG). High-quality images of the mono- and multilayers could be observed by STM after annealing. Monolayers of monomer were highly ordered showing orientational and positional correlation of alkyl side chains. Mixtures of pyrroles with different side chain lengths showed phase separation. Polymer monolayers showed high positional and orientational order and increased side chain packing density with side chain orientation more orthogonal to the surface. Polymer multilayers showed disorder, revealing connectivity and curvature of polymer chains. From the structures observed on solid substrates (gas-solid interface) conclusions are drawn for the polymerization process and the packing of molecules on the Langmuir-trough (at the gas-liquid interface).

## Introduction

Restricting monomer molecules to monolayers at planar surfaces during polymerization yields ordered anisotropic polymer thin films. Additionally, as the resulting polymer chains are prohibited from overlapping, the monolayer formed is highly two-dimensional (2-D). This type of ordered polymerization can be done at solid-liquid, liquid-liquid or gas-liquid interfaces.[1,2,3] Polymerizations at solid interfaces, however, are limited by the slow lateral diffusion of monomer and even slower diffusion of oligomer and polymer, which finally limits the size of the molecule. For a fluid interface, diffusion is much faster and when the applied surface pressure is maintained constant, limited conversion due to lateral shrinkage is not a problem. Although orientation at the aqueous surface greatly reduces the number of conformations the chains can assume, many possibilities still exist. These are described in the model of a "true self avoiding walk," that was originally used for modeling the adsorption of polymers onto solid substrates without allowing overlapping of chains. Since the adsorption process is analogous to chain growth during polymerization at the interface, this model can directly be applied for the description of the conformations of a growing polymer chain.[4] Besides the random walk of the chain growth at the interface other factors contribute to the packing of the molecules including phase separation of monomer, oligomer, and polymer, viscosity of the film, and polymer backbone stiffness, which all can be combined into kinetic and thermodynamic contributions.

No direct experimental observations have been reported to prove the two-dimensional order of LB-polymer films on water. Furthermore, although many types of 2-D polymerizations at gas-liquid interfaces (Langmuir polymerizations) have been reported in the literature, no imaging data at the molecular scale exists describing the conformation of the resulting polymer chains, the packing of the chains and the organization of the domains.

By introducing an electron rich monomer, which electrons are easily removed as they are close to the Fermi level, and a conductive polymer we report on scanning tunneling microscopy (STM) investigations of 2-D polymerized monolayers. The goal is to elucidate the packing of the monomer and the main chain conformation of its polymer.

<Insert Figure 1 about here>

3-Decyl pyrrole, 3-hexadecyl pyrrole and its polymer were used for these investigations as they form monolayers at the aqueous interface and can be transferred to solid substrates.[5,6,7] We will compare the ordering observed in monolayers of monomer, mixtures of monomers, polymer, and polymer multilayers, all which were transferred to molybdenum disulfide ($MoS_2$) or highly oriented pyrolytic graphite (HOPG) substrates and then annealed.

$MoS_2$ was chosen because the anchoring structures on it tend to reflect the intrinsic ordering of adsorbates because of its six-fold symmetry.[8] It also provides better STM contrast conditions that give brighter images of molecules containing long alkyl chains and is molecularly smooth without dangling bonds. HOPG was chosen as a second substrate, because it is well studied and gives a different STM contrast for alkyl chains and a different anchoring structure.

STM has proven to be a powerful tool for studies of the conformation of low molecular weight adsorbates on solid substrates. Furthermore, it has been used to study packing in transferred Langmuir-Blodgett (LB) monolayers,[9] however, limited molecular information could be gathered. This limited information has been attributed to the poor conductivity of the LB layer, a direct consequence of molecular packing orthogonal to the substrate plane. As a result, atomic force microscopy has been used more often to image LB films.[10,11] In our case, the intrinsic conductivity of the polypyrrole backbone and the pyrrole ring in the monomer should change the contrast and allow us to image both monolayers and multilayers by STM more successfully than conventional LB materials.

## Experimental and Chemicals

Synthesis of the monomers, 3-decyl pyrrole and 3-hexadecyl pyrrole, was based on previously published procedures.[12] Both compounds were found to be pure by $^{1}H$- and $^{13}C$-NMR (XL-200 NMR, Varian), TLC and FTIR. Elemental analysis of 3-hexadecyl pyrrole was as follows: calc. C=82.98, H=12.19, N= 4.84%; found C=82.62, H=12.74, N= 4.76%, respectively.

Monolayers of the monomers and the polymer were studied with a commercially available computer controlled film balance (KSV-5000, KSV Instruments, Finland). The interfacial pressure was monitored by suspending a platinum plate through the interface and applying the Wilhelmy method with on-line data acquisition through a surface balance. Monolayers were obtained by spreading a solution of the monomer dissolved in chloroform (ACS Spectro Grade, Eastman) at concentrations of approximately *0.5 mg/ml*. The balance was zeroed before addition. Isotherms of surface pressure versus mean molecular area per repeat unit (Mma) were measured at 23°C on Milli-Q® water with a resistance of greater than 18 MΩ/cm for the monomers. For polymerization and studies of the polymer, subphase solutions were made with A.C.S. reagent grade chemicals and Milli-Q® water. Subphase oxidizing agents were ferric chloride (0.03 M) or ammonium peroxodisulfate (0.03 M). After polymerization, materials collected from the trough surface for further analysis were washed with water dissolved in chloroform and after evaporation dried in a desiccator.

For STM-studies the polymerized monolayers were transferred directly after the two-dimensional polymerization applying Langmuir-Blodgett (vertical dipping) or Langmuir-Schäfer technique (horizontal dipping). The layers were deposited on freshly cleaved $MoS_2$ (Hori Mineral Co.) and HOPG (Union Carbide), with a KSV mini-trough. Conditions for transfer were room temperature (21°C), substrate dipping speed 5 to 10 mm/min with a surface pressure for transfer of 20 mN/m.

Monolayer samples were prepared by one upstroke of the substrate through the interface, placing the hydrophilic pyrrole rings or the polypyrrole backbone at the substrate surface, as well as by one downstroke and a high speed upstroke with negligible transfer observed, putting the alkyl chains onto the solid surface. Multilayer samples were prepared by alternating up and down strokes through the interface. The horizontal transfer was done by lowering the substrate with a micrometer screw. With this technique only monolayer samples were prepared.

STM pictures were obtained on a NanoScope II® in the constant current mode in air. Tip bias voltages ranged from 1100 to 1600 mV for the monomer and -765 to -1980 mV for the polymer, tunneling currents ranged from: 0.09 to 0.37 nA, tips (Pt-Ir) were bought from Digital Instruments, CA, and recut with scissors as needed. To achieve high resolution images, samples were annealed for at least twelve hours above the melting temperature of the monomer before investigation. Then, they were allowed to cool down at a rate of 5°C per 15 min with a pause of 45 min close above the melting temperature of the monomer. To modify the different anchoring structures for some polymer monolayers, a drop of chloroform was spread with a Hamilton syringe onto the substrate while scanning.

## Results and Discussion

### Monomer and polymer at a gas-liquid interface

< Insert Figure 2 about here >

The isotherm of 3-hexadecyl pyrrole is depicted in Figure 2. On a pure water surface, the onset of the isotherm is at a Mma per molecule of 26.5 Å$^2$. Its collapse pressure is 63 mN/m. Before collapse, a highly viscous film is observed that can move the Wilhelmy plate when working on a single barrier trough. By adding ammonium sulfate to the subphase no change in the isotherm can be observed up to concentrations of 0.03 M. The same has been reported for ferric chloride in concentrations up to 0.01 M.[7] However, concentrations of 0.05 M and higher of ferric chloride showed a change. The observed increase in surface area can be interpreted as a phase transition from a liquid condensed to a liquid expanded layer. The same type of phase transitions have been reported by Herrington.[13]

The amphiphilic molecule is thought to place itself according to its polarity and to the polarity of the interface, i.e., the more polar pyrrole group is in the water whereas the alkyl chain points into the air. From the tangent of the isotherm the mean molecular area of one molecule at zero surface pressure can be measured as 22.6 Å$^2$. With a few simple assumptions the average arrangement of the molecules at the surface can be estimated. First, the molecules are considered to be rigid rods. Second, they form a dense packing on a surface and, third, the rods have a diameter of 0.36 nm. An average tilt angle to the surface of 72.2° can then be calculated.

A 2-D polymer can be formed by polymerizing the monomer 3-hexadecyl pyrrole with an oxidizing agent in the subphase. During polymerization the monomer reacts by forming bonds and, therefore, brings the molecules closer together. This can be observed macroscopically by the decrease in surface area, when polymerization is done at constant surface pressure. After polymerization the monolayer can be expanded and compressed, which is shown in Figure 2. The collapse pressure for the polymer film is lower compared to the monomer and the tightly collapsed film is dark colored with molecular weight averages of 3500 to 6000 measured by GPC using polystyrene standards. The point of onset in the first compression curve of the polymer is at a larger Mma than for the monomer isotherm. This seems to be contradictory since during polymerization, the Mma of the monolayer decreased. This apparent contradiction can be explained by the following. First, the monomer isotherm is dependent on the salt concentration and type of salt in the subphase, as discussed above. Second, after polymerization the monolayer will rearrange and demix on decompression, simultaneously allowing the pyrrole group to lie more flat on the surface. Hysteresis experiments indicate that this is the case since on repeated compression-decompression cycles the isotherm reaches a constant value that is equivalent to the value directly after polymerization.

Transfer onto substrates is possible with transfer ratios being about unity.[6] For more experimental details about the Langmuir polymerization of 3-hexadecyl pyrrole we refer to the existing literature.[5,6,7,14]

## Monomer at a gas-solid interface

Images of a 3-hexadecyl pyrrole monomer monolayer at the $MoS_2$-air interface obtained by STM are shown in Figure 3. The dimensions of the pictures are 15 nm by 15 nm. Rod-like structures are observed showing high orientational and positional order. The rods form rows with a row-to-row distance of about

1.5 nm and are tilted at an angle of 40° to the rows. The measured rod length is 1.7 ± 0.1 nm, and the thickness about 0.36 nm. Additionally, it is clear from the image that the rods are interdigitated, i.e., the end of one rod lies in between two other rods of the next row.

< Insert Figure 3 about here >

The rod-like structures can be correlated with monomer molecules. Each rod corresponding to one molecule. Applying the simple model with cylindrical rod like molecules (molecular width 0.36 nm and length 2.06 nm) in a dense packed structure, an angle to the surface of 12.2° can be calculated. The width of the rods of 0.36 nm can be deduced from the STM measurement. The assumption of a stiff rod-like all-trans alkyl chain may be expected for a hexadecyl chain which is likely to crystallize. Furthermore, the images suggest that this might be so.

This result implies that at an angle of 12.2° only 17.4 nm of the molecule is visible as demonstrated in Figure 4B. By using bond distances, however, the calculated length of 3-hexadecyl pyrrole is about 2.06 nm, therefore, about 0.32 nm of the molecule is covered and cannot be seen by the STM-tip. To distinguish which part of the molecule it is, the hexadecyl chain or the pyrrole ring, experimental parameters were changed while scanning the same area. An electron rich pyrrole ring, where electrons are closer to the Fermi level than in alkyl chains is expected to show different tunneling conditions than alkyl chains. If the pyrrole group was in the visible part of the molecule, a change in the tunneling conditions should show a different contrast for some part of the rod-like structure. In fact, an overall change can be observed, but no features in the rod-like structure could be identified that could be correlated with the ring. Therefore, we conclude that the pyrrole ring is not visible and must be attached to the substrate.

Additionally, the observed packing distances do not allow the ring to lie flat on the substrate; the ring must be standing. The attachment of the ring is also expected from the transfer method; an upstroke places the hydrophilic pyrrole ring on the substrate surface and the alkyl chains in the air. Annealing above the melting temperature of the bulk might cause a complete reorganization, but it is also thermodynamically expected that the more polar ring should be adsorbed on $MoS_2$ and the less polar alkyl chains at the air surface form a low energy surface.[15]

< Insert Figure 4 about here >

## Comparison of 3-hexadecyl pyrrole monolayers at a liquid-gas and a solid-gas interface.

The mean molecular area on water is 22.6 Å², whereas that on $MoS_2$ is 57 Å². The increase in surface area per molecule of 34.4 Å² implies that during annealing, about half the molecules must be extruded from the monolayer. Some differences in the molecular arrangement of the monolayer at the liquid-gas and solid-gas interface are shown in Figure 4. The angle formed by the alkyl chain on water and $MoS_2$ is calculated to be 72.2° and 12.2°, respectively. It should be mentioned that no surface pressure is externally applied to the monolayer at the solid surface, whereas the freedom of the molecules in the layer at the liquid interface is mechanically restricted by a barrier.

No images could be obtained when samples were scanned directly after deposition, without annealing. Since STM, as we used it, did not allow the detection of very irregular structures on a molecular scale, we assume that the monolayer directly after deposition is not well ordered. The layer had to be annealed above the bulk melting point to allow for an ordered thermodynamically stable monolayer structure to form.

Therefore as used here, LB transfer is only a tool that allows for convenient and relatively uniform initial film thickness in the nanometric scale, not to establish the nature of the lateral packing of the molecules. It should be also noted that melting and diffusion of a few micrograms of 3-hexadecyl pyrrole on $MoS_2$, a common sample preparation method for STM observation of other low molecular weight organics did not give monolayers which were observable by STM.[16]

## Mixtures of 3-decyl pyrrole and 3-hexadecyl pyrrole

Scanning pure 3-decyl pyrrole monolayers always resulted in images of the clean $MoS_2$ surface. Bulk 3-decyl pyrrole is a liquid at room temperature, its melting temperature being 16.5°C. Therefore, it is expected that the compound is moved easily by the tip while scanning the surface.

Scanning mixtures of 3-decyl pyrrole and 3-hexadecyl pyrrole gave the images shown in Figure 5. A mixture of 5% 3-decyl pyrrole in 95% 3-hexadecyl pyrrole was transferred in an upstroke from the water surface onto $MoS_2$. The STM images in Figure 5 A and B show a region of 13.5 nm squared.

<Insert Figure 5 about here >

Clearly separated domains of different rod like structures can be recognized in all images. Again, we assume that each of these rods corresponds to one molecule. Since mixtures were scanned, it is not clear which rod corresponds to each monomer. The length of the rods observed by the STM tip ranges from 1.2 to 1.9

nm. Since we cannot directly correlate the rods with the type of molecule, no angles of attachment with respect to the substrate layer plane can be calculated. The different measured rod lengths may correspond to the same type of molecule attached at a different angle. They also may correspond to different monomers attached at different angles. Generally, most of the rods are assumed to correspond to the 3-decyl pyrrole, since its spreading ratio was 95 %. The ratio is very likely to shift to higher values for the hexadecyl pyrrole because the decyl pyrrole is slightly soluble in water and will diffuse to a certain extent into the subphase before transfer. Additionally, the decyl substituted compound is a liquid in the bulk and can be moved easily by the tip at the surface. The structures observed by the tip, therefore, have to be thermodynamically stable, i.e., only smaller domains of the shorter alkyl chain compound that are stabilized by domains of the hexadecyl compound or mixtures of the compounds or domains of different mixtures will be visible. The structures that can be found on these samples are shown in Figure 5 .

Figure 5A shows a region where formation of domains occurs. These domains consist of mixtures with different amounts of the hexadecyl and decyl compound. We can conclude this because we find rod like structures ranging from 1.2 to 1.9 nm in all domains. 3-Decyl pyrrole lying completely flat would only allow a length of 1.4 nm and a pure 3-hexadecyl pyrrole would show the packing seen in Figure 3. Additionally, there is not enough 3-hexadecyl pyrrole transferred to cover the surface with such a dense packed monolayer.

Figure 5B shows a region of the same sample with 2 domains. On the left side of the image, a domain with rows of molecules having positional and orientational order is seen. On going to the center, the positional order is reduced, while the orientational order is retained resulting in a 2-D nematic-like ordering. No interdigitation is observed either in the region with rows or in the 2-D nematic phase region.

The image in Figure 5C shows a region of the size 18.75 nm that is ordered in rows with a row to row distance of 0.75 nm and no interdigitation of the rods. We expect this region more likely to be pure 3-decyl pyrrole because of the different packing structure. The image in Figure 5D was scanned in the same region with a higher magnification. The image is 6.75 nm squared. The rods that can be seen have a length of 1.4 nm and form an angle of 32° to the rows. If we assume that this is a pure 3-decyl pyrrole region and apply the rigid rod model, we can conclude that the molecules have to lie completely flat on the surface because the length of the rods equals the length of 3-decyl pyrrole. This implies that the dark area at the end of the rod that indicates a thinner overlayer or good conductivity is very likely to be the pyrrole ring. The length of this black part equals 0.32 nm which is exactly the amount that is not visible in the packing structure of pure 3-hexadecyl pyrrole.

Overall we can conclude the following from the mixtures of monomer. Different types of packing structures are possible. Packing is possible in domains with positional and orientational order with and without interdigitation with mixed domains tending toward structures with loss of positional order, only keeping one major axis of order, i.e., 2-D nematic phase formation. The packing of the molecules seems to be highly influenced by the surface structure of the substrate. The minimization of surface energy for the monolayer that leads to coverage of the pyrrole group by the alkyl chains in the hexadecyl compound is overruled by the enthalpic adsorption onto the sites along one of the major axis of the substrate surface for the decyl compound, which is a liquid in the bulk.

## Polymer monolayers at gas-solid interfaces

Poly (3-hexadecyl pyrrole) was transferred via vertical deposition on HOPG (Fig. 6A), vertically in one upstroke or one downstroke on $MoS_2$ (Fig. 6B and C, respectively) and horizontally on $MoS_2$. Furthermore, the horizontally deposited monolayer was solubilized with chloroform while scanning and higher resolution images (Fig. 6 D, E, F) could be obtained after evaporation.

< Insert Figure 6 about here >

Figure 6A shows a STM image of poly (3-hexadecyl pyrrole) on HOPG. Rod like structures can be seen that form an ordered structure in rows. The row to row distance being 0.59 nm. The rods form an angle of 27° with the rows. A Mma of 32 Å² can be calculated that compares well to the monolayer at the liquid interface.

Scanning a vertically dipped polymer monolayer on $MoS_2$ gives the images as shown in Figure 6B. Rod like structures organized in rows with a row to row distance of 0.9 nm and a rod length of 1.4 nm leading to an angle of 40° and a Mma per repeat unit of 49 Å² can be seen. The same structure is observed for polymer monolayers that were transferred with one downstroke and then annealed (Fig. 6C). The annealing, therefore, appears to change the orientation of the deposited film, placing the polymer backbone at the substrate surface.

Horizontal dipping and annealing leads to comparable structures as the vertical deposition. However, after spreading a drop of chloroform while scanning, a new packing with lower density can be observed. A Mma per repeat unit of about 60 Å² resulted. Furthermore, faint streaks at the end of each rod and in the row direction may be due to the presence of the polymer backbone. In any case, the chloroform appeared to "swell" the polymer monolayer, attaching the backbone to a major axis of orientation of the substrate.

The polymer ordering was observed on $MoS_2$ over a wide range of scanning conditions, tip bias voltages, both positive and negative between 700 mV and 2200 mV and tunneling currents between 0.07 to 1,0 nA. The above behavior is in contrast to the monomer, where increasing the tunneling current or changing the tip bias voltage toward zero easily resulted in molecules being scraped off by the tip, revealing the underlying $MoS_2$ lattice.

Independent of substrate and transfer protocol, the following features can be observed, that provide useful information for comparison with the monomer monolayers. Similar rod-like structures are observed that display orientational alignment perpendicular to the scanning direction. Each rod-like structure may correspond to a single alkyl side chain along the polymer backbone. The backbone is not clearly visible, perhaps only becoming partially visible upon swelling by chloroform. The side chain packing density in the polymer monolayer on graphite is greater. This suggests that the anchoring interactions on graphite are weaker than those on $MoS_2$ and polymer-polymer interactions, much like that at high applied surface pressure on the water surface, dominate the anchoring structure formation on graphite. The increased side chain density on $MoS_2$ is related with two structural distances. The first is the chemically defined repeat distance determined by the chemical bonds and configuration of the underlying polymer backbone. The second involves the proximity of one polymer chain to another.

< Insert Figure 7 about here >

On $MoS_2$, the alkyl side chain ordering observed in the polymer image can be explained by an all-transoidal conformation of the (polymer all transoidal conformation of a 2,5 head to tail condensation) polypyrrole backbone with respect to the nitrogen, such that each polymer chain arranges its alkyl side chains into two parallel rows. In this conformation, the distance between these two parallel rows of alkyl side chains corresponds to nearly twice the $MoS_2$ lattice spacing. Polymer main chains are then aligned in a parallel fashion suggestive of the overall conformation depicted in Figure 7. If the distance between the polymer main chains is also twice the $MoS_2$ lattice spacing, then this conformation very accurately explains the uniform structure and the two directions of row alignment observed in the STM images.

We suppose there are several reasons that lead to the observed polymer anchoring structure on $MoS_2$: The backbone oriented parallel to a major axis of $MoS_2$ reduces the interfacial energy, the backbone at the $MoS_2$ and side chains extended toward the air reduce the surface energy. The parallel alignment of adjacent polymer chains and that of the alkyl side chains allows for the best packing density at the surface. Similar anchoring induced ordering has been observed for systems of low molecular weight rod-like molecules[16] such as cyanobiphenyl containing liquid crystals.

## Polymer multilayers

Figure 8A-B shows STM images of a polymer multilayer. Rod-like structures are seen that may correspond to the alkyl side chains. The alkyl side chains no longer show very high orientational correlation and they do not uniformly orient perpendicular to the scanning direction. Generally an increase in disorder is observed. The rows of alkyl side chains are existing but curvature is visible, which gives evidence of connectivity between them. Each polymer chain still shows positional row correlation but the chains now appear to "drape" themselves over defects in the layers below and to show curvature in the layer plane. Inter-row distances also show local variations not observed in the monolayer images.

<Insert Figure 8 about here>

The multilayer structure observed may be described as follows. The innermost layer against the $MoS_2$ surface is very highly ordered with the polymer backbone oriented directly against the substrate surface. Subsequent overlayers are much more disordered, and more closely reflect the polymer backbone conformation after polymerization at the gas-liquid interface. The long alkyl chains of the first and second layer can be compared to as solvent for the overlayer, therefore, also changing the surface characteristic from a solid to a more liquid-like one.

The effects of the annealing process in monolayers of both the monomer and polymer can be compared. Both systems required annealing in order to achieve very high molecular resolution by STM. This emphasizes the importance of molecule-substrate interactions in defining surface order. However, the degree which annealing affected the two systems was very different. As discussed earlier, the monomer showed a tendency to be easily reordered from its original packing in the LB-layer by extrusion of some molecules from the surface. For the polymer, respacing and realignment of the polypyrrole backbone with a major axis of the $MoS_2$ occurred, but generally the layer showed a greater stability associated with higher molecular weight molecules and therefore, more anchoring sites.

Very ordered structures with both orientational and positional correlation can be seen in all monomer and polymer images. For the monomer, the annealing process allows the molecules to orient parallel to the surface, whereas for the polymer, the backbone becomes aligned parallel with a major axis of the $MoS_2$ substrate and establishes positional order. Thus both the positional order and chemical repeat distance define the side chain packing density. As an effect, the side chains cannot align parallel to the solid surface as in the monomer monolayers. They remain partially erect due to steric interactions with adjacent side chains. In both cases, a significant degree of ordering is induced.

The polymer backbone in the outer layer of the multilayer system is not orientationally ordered by the $MoS_2$. It can take up conformations much more alike those intrinsic to the polymerization at the gas-liquid interface. The molecular conformation or contrast conditions allow to observe even greater evidence of the connectivity related to the backbone. The long alkyl side chains of the underlying monolayers serve as solvent for the top layers. Therefore, the conformation of the top layers shows increasing disorder compared to the first layer which order appears to be highly dependent on the molecule-substrate interactions.

The observed images on solid substrates suggest the following conclusions about the monolayers and the polymerization process at the air-liquid interface. The nematic-like domain formation by small oligomer molecules must compete with the tendency for a polymer chain to phase separate as a single unit or to fold back and forth across itself.[17] The last two conformational possibilities demand a greater degree of polymerization. At the gas-liquid interface, then, rapid domain formation by small oligomer molecules is possible and would likely favor conformations dominated by parallel alignment of the polymer chains. Thus, the fluidity of the gas-liquid interface may amplify the rate dependence of the resulting polymer conformations compared to those observed at a solid surface.

## Conclusions

The Langmuir trough and the LB technique were used as tools for establishing quasi two-dimensionality during polymerization and uniform film thickness; not to define local lateral order within a layer transferred to $MoS_2$ as has been shown.

For mixtures of monomers phase separation with domain formation can be concluded. It also can be concluded that the ordering of the monomer on $MoS_2$ is caused by organization parallel to a major axis of the lattice. For the polymer, the ordering of the backbone along a major axis of the lattice forces the side chains into a different packing than in the monomer. The structures seen are regularly ordered giving evidence that the polymer formed is highly regular 2,5 head to tail and in an all-transoidal conformation. This suggests that during the polymerization process, the dense packed monomer monolayer mainly allows polymerization in the 2,5 position.

Another important result of these investigations was that the introduction of a conductive polymer backbone did allow the imaging of both, LB monolayers and multilayers successfully. Such conducting polymers are candidates for a new class of adsorbates to flexibly modify $MoS_2$ and other substrates. Thus, using conductive polymer films as underlayers to change lattice spacing or contrast conditions may prove useful for studying other systems such as alignment in liquid crystals or functional group effects in molecule-molecule interactions.

## Acknowledgment

The Deutsche Forschungsgemeinschaft and the Office of Naval Research are acknowledged for support.

## Figure Captions

Figure 1 Chemical structures of the monomer (A) 3-hexadecyl pyrrole and its polymer (B) poly (3-hexadecyl pyrrole).

Figure 2 Surface pressure vs. mean molecular area during compression for 3-hexadecyl pyrrole (A) on water and poly (3-hexadecyl pyrrole) (B) on 0.03 M ammonium peroxodisulfate subphase solution. Temperature 23°C, surface pressure for polymerization 10 mN/m. Compression barrier speed 20 mm/min.

Figure 3 STM samples were prepared by vertical transfer of preformed monolayers to $MoS_2$ substrates. STM images of 3-hexadecyl pyrrole monomer on $MoS_2$ scanned in constant current mode at room temperature in air. Monolayers transferred vertically in upstroke from pure water subphases onto fresh cleaved $MoS_2$. Dimensions of the pictures: (A and B) 15 nm x 15 nm, tip bias voltage 1320 mV, current 0.31 nA.

Figure 4 Pictorial model calculated from the observed packing of monolayers of 3-hexadecyl pyrrole. The rigid rods have a length of 2.06 nm and a diameter of 0.36 nm. Organization at (A) the air-water interface and, (B) the $MoS_2$-air interface.

Figure 5 STM images of a mixture of 3-decyl pyrrole and 3-hexadecyl pyrrole monomer monolayers on $MoS_2$. Dimensions of pictures: (A and B) 13.5 nm x 13.5 nm, tip bias voltage -1364 mV, current 0.12 nA; (C) 18.75 nm x 18.75 nm, tip bias voltage -1364 mV, current 0.13 nA (D) 6.75 nm x 6.75 nm, tip bias voltage -1364 mV, current 0.13 nA.

Figure 6 STM images of poly(3-hexadecyl pyrrole) monolayers in constant current mode in air. Substrate, type of deposition and dimensions for images: (A) HOPG, vertical upstroke, size 10 nm x 10 nm, tip bias voltage -765 mV, current 0.37 nA; (B) $MoS_2$, vertical upstroke, size 7 nm x 7 nm, tip bias voltage -1400 mV, current 0.2 nA; (C) $MoS_2$, vertical downstroke, size 10 nm x 10 nm, tip bias voltage 1599 mV, current 0.13 nA; (D) $MoS_2$, horizontal deposition, $CHCl_3$, size 6 nm x 6 nm, tip bias voltage -1362 mV, current 0.23 nA; (E) $MoS_2$, horizontal deposition, $CHCl_3$, size 6 nm x 6 nm, tip bias voltage -1362 mV, current 0.23 nA; (F) $MoS_2$, horizontal deposition, $CHCl_3$, size 6 nm x 6 nm, tip bias voltage -1362 mV, current 0.14 nA.

Figure 7 Pictorial model of the polymer monolayer structure observed at the $MoS_2$-air interface without swelling by $CHCl_3$. Alignment with double spacing of the $MoS_2$.

Figure 8 STM images of polymer multilayers. (A-B) poly(3-hexadecyl pyrrole). The sample was prepared from a mixed monolayer containing 64% of the low molecular weight liquid crystal 8CB, used as a processing aid and to establish additional disorder at the surface. Note the polymerization was carried out prior to the addition of 8CB. The samples were prepared by vertical deposition at an applied pressure of 8 mN/m and were nominally 3 layers thick. The samples were annealed after transfer of all layers. Dimensions of images: (A) and (B) 10 nm x 10 nm, tip bias voltage -1980 mV, current 0.14 nA.

## References

1. Gaines, G. L. *Insoluble Monolayers at Liquid-Gas Interfaces* (Wiley, New York, 1966), pp. 321-2.
2. Sigmund, W. M.; Duran, R. S. *Macromolecules* **1993**, *26*, 2616.
3. Ulman, A. *An Introduction to Ultrathin Organic Films: From Langmuir-Blodgett to Self-Assembly* (Academic Press, **1991**), 176-185.
4. Bulgadev, S.; Obukov, S. *Sov. Phys. JETP* **1984**, *59*, 1140.
5. Duran, R. S.; Zhou, H. C. *Polymer* **1992**, *33*, 4019.
6. Sigmund, W. M.; Marestin, C.; Keil, S.; Zhou, H.; Elsabee, M. Z.; Rühe, J.; Wegner, G.; Duran, R. S. *Macromolecules*, submitted **1993**.
7. Rahman, A. K. M.; Samuelson, L.; Minehan, D.; Clough, S.; Tripathy, S.; Inagaki, T.; Yang, X. Q.; Skotheim, A. T.; Okamoto, Y. *Synth. Met.* **1989**, *28*, C237.
8. Iwakabe, Y.; et al., *Jap. J. of Appl. Phys.* **1991**, *30*, 2542.
9. Smith, D. P. E.; et al. *Proc. Natl. Acad. Sci. USA* **1987**, *84*, 969.
10. Zasadzinski, J. A. N.; et al., *Biophys. J.* **1991**, *59*, 755.
11. Schwartz, D. K.; Garnaes, J.; Viswanathan, R.; Zasadzinski, D. P. E. *Science* **1992**, *257*, 508.
12. Rühe, J.; Ezquerra, T. A.; Wegner, G. *Makromol. Chem. Rapid Commun.* **1989**, *5*, 1.
13. Herrington, T. M.; Aston, M. S. *J. Colloid Interface Sci.* **1991**, *141*, 50.
14. Hong, K.; Rosner, R. B.; Rubner, M. F. *Chemistry of Materials* **1990**, *2*, 82-88.

15. Koopman, D. C.; Gupta, S.; Ballamudi, G. B.; Westermann-Clark, G. B.; Bitsanis, I. A. *J. Chem. Phys.*, submitted **1993**.

16. Hara, M.; et al. *Nature* **1990**, *344*, 228.

17. Onsager, J. *Ann. N.Y. Acad. Sci.* **1949,** *51*, 627.

Figure 1 -- Parts a and b

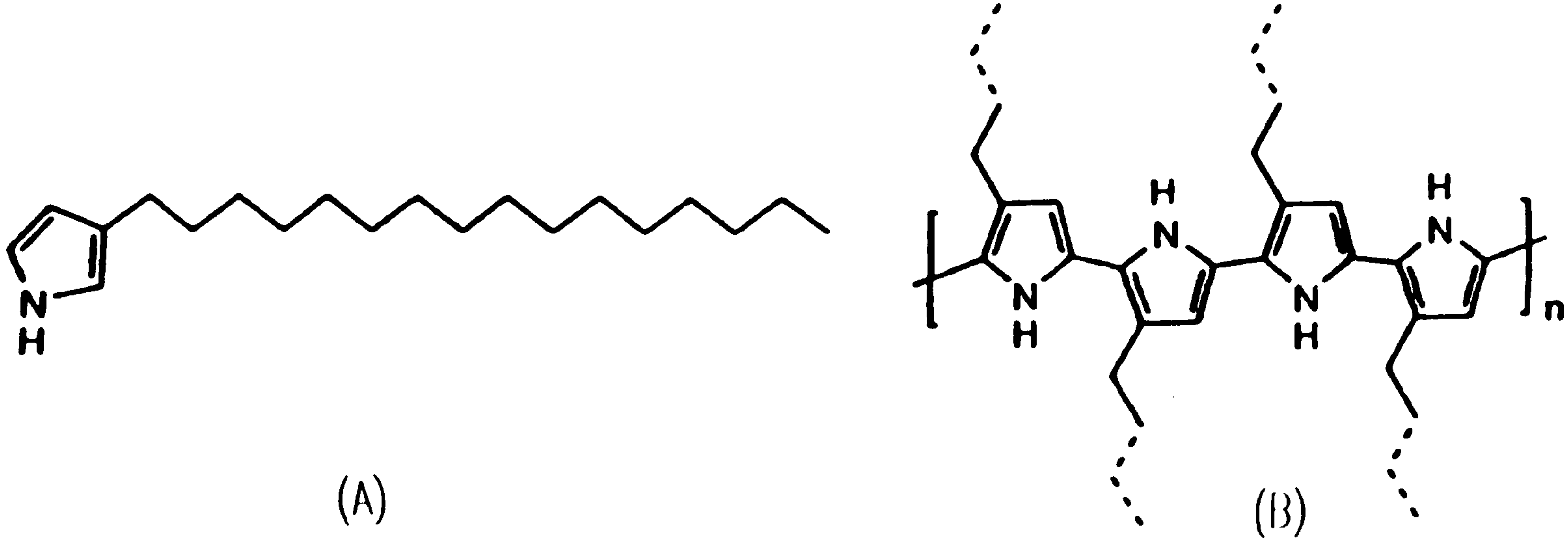

(A) (B)

Figure 2

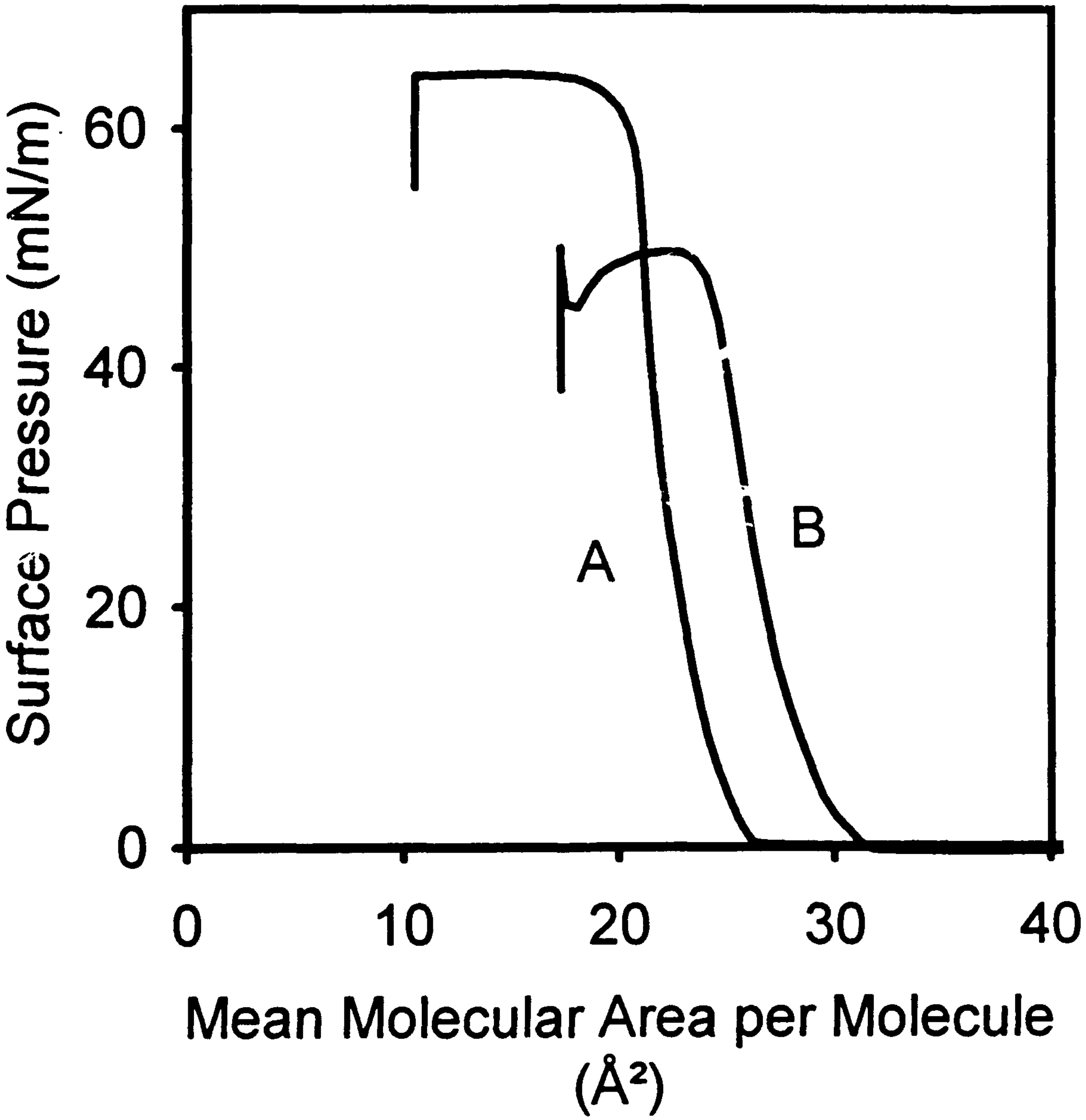

Surface Pressure (mN/m)
60
40
20
0
A
B
0
10
20
30
40
Mean Molecular Area per Molecule
(Å²)

Figure 3 -- Parts a and b

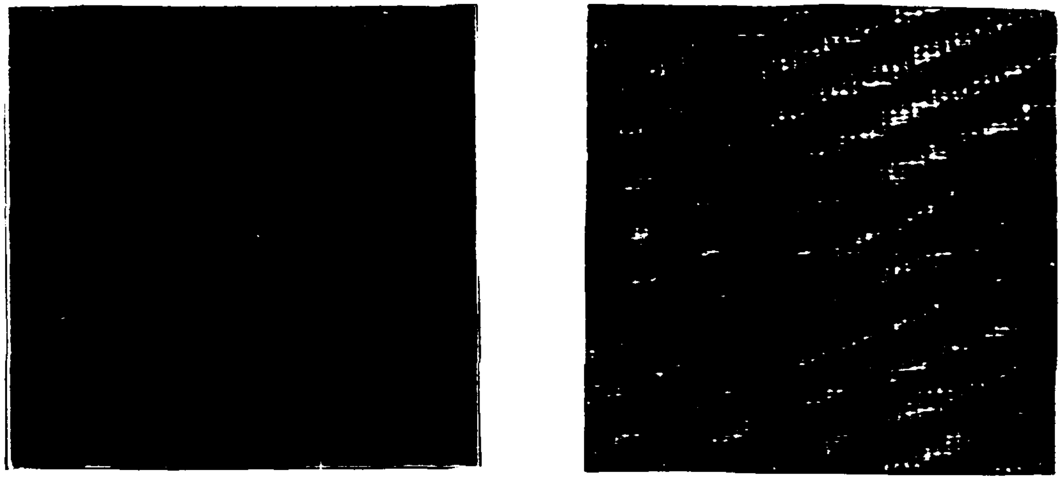

(a)

(b)

Figure 4 -parts a and b

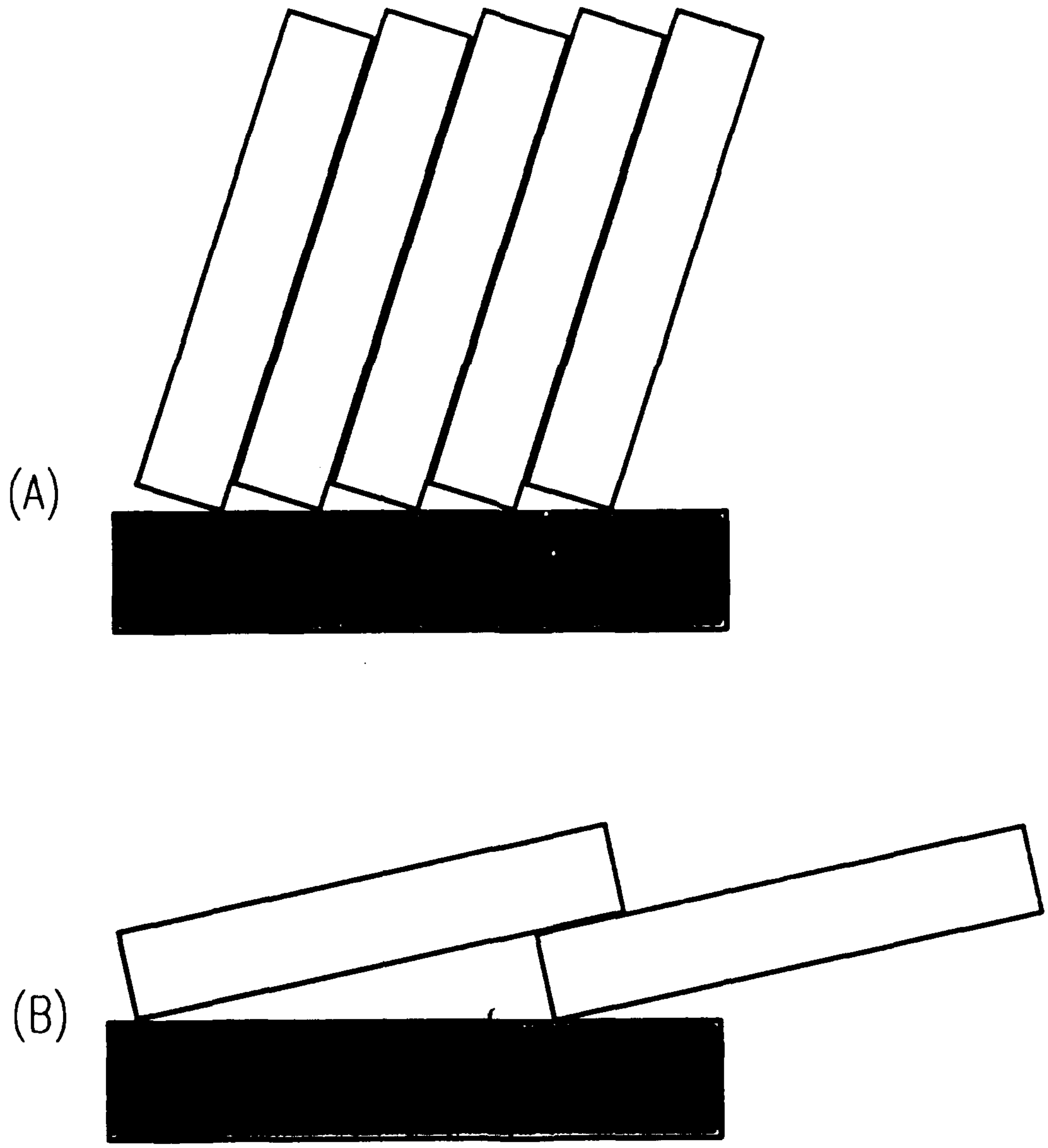

Figure 5 -- Parts A, B, C and D

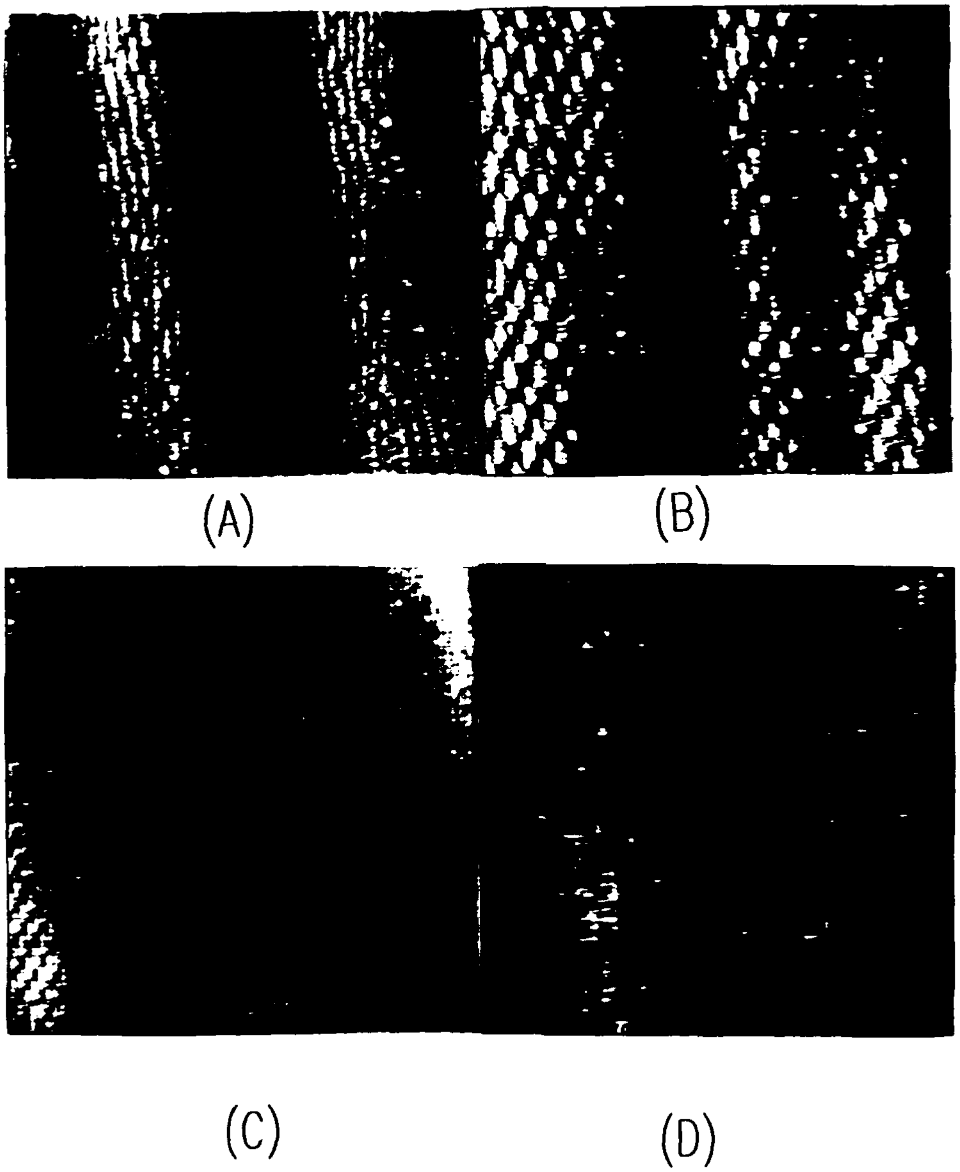

Figure 6 -- Parts a, b, c, d, e, f

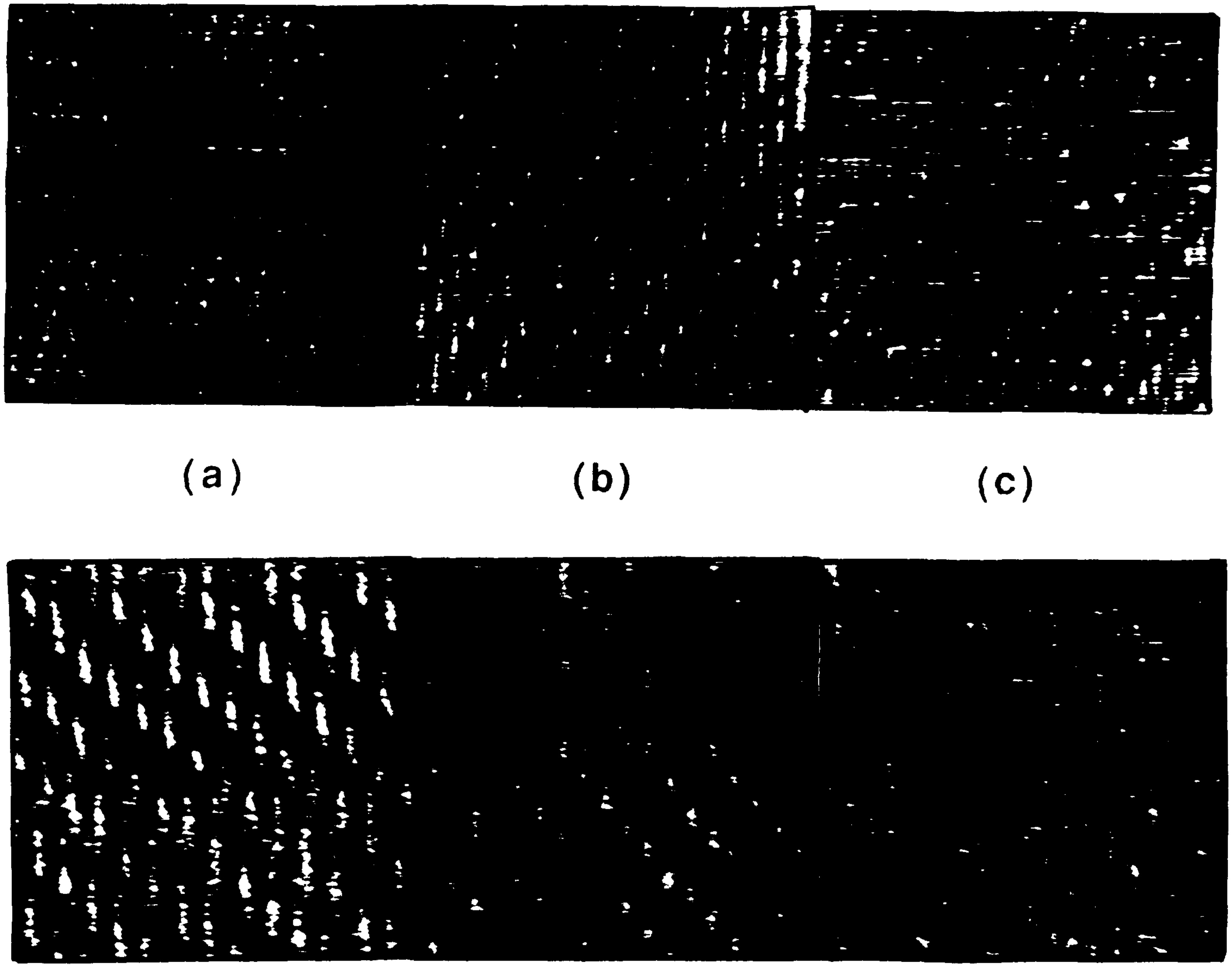

(a) (b) (c)

(d) (e) (f)

Figure 7

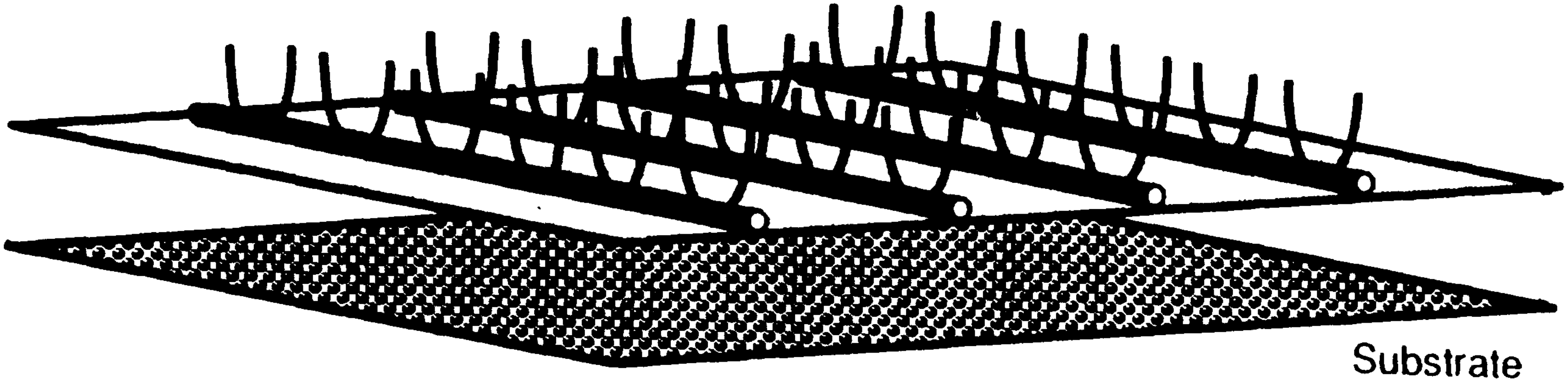

Figure 8 -- Parts a and b

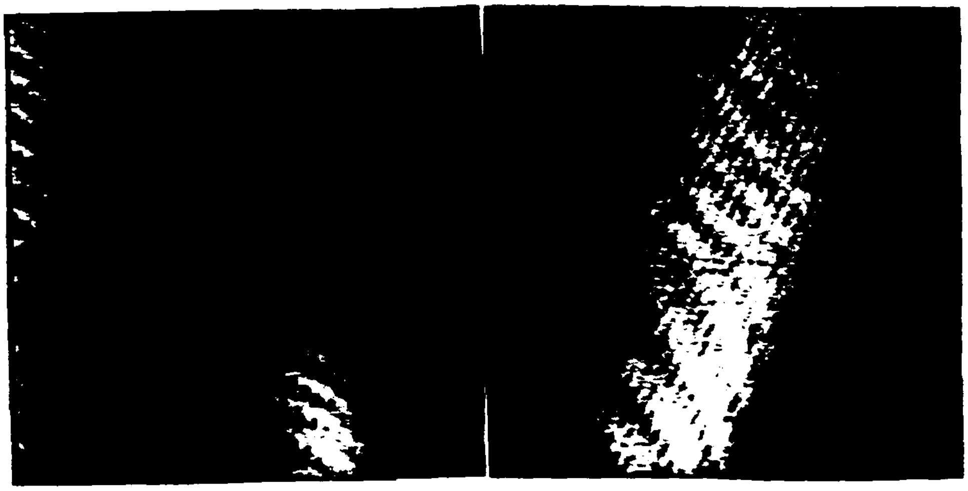

(a) (b)

# TECHNICAL REPORT DISTRIBUTION LIST - GENERAL

Office of Naval Research (2)*
Chemistry Division, Code 1113
800 North Quincy Street
Arlington, Virginia 22217-5000

Dr. James S. Murday (1)
Chemistry Division, Code 6100
Naval Research Laboratory
Washington, D.C. 20375-5000

Dr. Robert Green, Director (1)
Chemistry Division, Code 385
Naval Weapons Center
China Lake, CA 93555-6001

Dr. Eugene C. Fischer (1)
Code 2840
David Taylor Research Center
Annapolis, MD 21402-5067

Dr. Elek Lindner (1)
Naval Ocean Systems Center
Code 52
San Diego, CA 92152-5000

Commanding Officer (1)
Naval Weapons Support Center
Dr. Bernard E. Douda
Crane, Indiana 47522-5050

Dr. Richard W. Drisko (1)
Naval Civil Engineering Laboratory
Code L52
Port Hueneme, CA 93043

Dr. Harold H. Singerman (1)
David Taylor Research Center
Code 283
Annapolis, MD 21402-5067

Chief of Naval Research (1)
Special Assistant for Marine Corps Matters
Code 00MC
800 North Quincy Street
Arlington, VA 22217-5000

Defense Technical Information Center (2)
Building 5, Cameron Station
Alexandria, VA 22314

* Number of copies to forward

Enclosure